Tunable emission in surface passivated Mn-ZnS nanophosphors and its application for Glucose sensing

Manoj Sharma, Tarun Jain, Sukhvir Singh, and O. P. Pandey

Citation: AIP Advances **2**, 012183 (2012); doi: 10.1063/1.3698310
View online: http://dx.doi.org/10.1063/1.3698310
View Table of Contents: http://aipadvances.aip.org/resource/1/AAIDBI/v2/i1
Published by the American Institute of Physics.

Tunable emission in surface passivated Mn-ZnS nanophosphors and its application for Glucose sensing

Manoj Sharma,[1,4] Tarun Jain,[2] Sukhvir Singh,[3] and O. P. Pandey[4,a]
[1]*Department of Nanotechnology, Sri Guru Granth Sahib World University, Fatehgarh Sahib-140407, Punjab, India*
[2]*Department of Biotechnology, Thapar University, Patiala-147 004, Punjab, India*
[3]*Electron Microscopy Division, National Physical Laboratory, New Delhi-110001, India*
[4]*School of Physics and Materials Science, Thapar University, Patiala-147 004 Punjab, India*

(Received 3 June 2011; accepted 15 February 2012; published online 23 March 2012)

The present work describes the tunable emission in inorganic-organic hybrid NPs which can be useful for optoelectronic and biosensing applications. In this work, Mn- ZnS nanoparticles emitting various colors, including blue and orange, were synthesized by simple chemical precipitation method using chitosan as a capping agent. Earlier reports describe that emission color characteristics in nanoparticles are tuned by varying particle size and with doping concentration. Here in this article tunable emission has been achieved by varying excitation wavelength in a single sample. This tunable emission property with high emission intensity was further achieved by changing capping concentration keeping host Mn-ZnS concentration same. Tunable emission is explained by FRET mechanism. Commission Internationale de l'Eclairage (CIE) chromaticity coordinates shifts from (0.273, 0.20) and (0.344, 0.275) for same naocrystals by suitably tuning excitation energy from higher and lower ultra-violet (UV) range. Synthesized nanoparticles have been characterized by X-ray diffraction, SEM, HRTEM, UV- Visible absorption and PL spectroscopy for structural and optical studies. Using tunable emission property, these highly emissive nanoparticles functionalized with biocompatible polymer chitosan were further used for glucose sensing applications. [http://dx.doi.org/10.1063/1.3698310]

I. INTRODUCTION

Semiconductor nanoparticles (NP's) exhibit tunable emission either by size selective synthesis or by doping suitable transition metal ions in wide band gap nanocrystals (NC's). These properties enable NPs to be used as lasers, flat panel displays, optical storage, single electron transistors and as biological probes.[1–4] CdSe and CdTe have been widely studied as tunable emitters due to their quantum size effect.[2,3] These NPs have been synthesized in the range of 2 to 20nm to obtain colors in the visible spectrum. But intrinsic toxicity of cadmium has created doubt for its end application.[5] Also many groups have studied various kinds of doped NC's for other applications.[5–13] Suitable doping in host NC's lattice can give different colors in visible region. Moreover, for sensing applications a suitable functional group is required for attachment of QDs with biological molecules. Considering this aspect a need is felt to search for a nanophosphor of non toxic nature to be used in sensing applications. Among all semiconductor nanomaterials, ZnS nanocrystals doped with transition metal ions such as Mn^{2+} have been regarded as a promising new class of nanophosphors, owing to their superior luminescent properties.[5–10] Also in these materials we can get various colors in visible

[a]Author to whom correspondence should be addressed. Electronic mail: oppandey@thapar.edu

region by doping ZnS with different transition metal ions.[10–12] However, as synthesized Mn^{2+} doped ZnS NC's usually suffer some problem such as poor quality of NC's and limited tunable emission color.[5] It is also reported earlier that by doping transition metal ions or rare-earth elements into ZnS NCs, the luminescence region can extend to the full UV–visible band. Bhargava *et al.*[13] first reported the preparation and photoluminescence (PL) properties of ZnS: Mn NCs. Thereafter, Mn^{2+} doped ZnS NCs become a favorable phosphor, contributing to the characteristic luminescence properties in orange region for potential applications in displays, sensors, and lasers.[13] In Mn^{2+} doped systems usually orange emission around 590 nm resulting from $^4T_1$–$^6A_1$ transition of the Mn^{2+} impurity excited by energy transfer from the ZnS host is observed. However, in all reports mentioned above many samples of different particle sizes (CdSe, CdTe etc.) or with different dopants (ZnS: Mn, ZnS: Cu, CdS: Mn, ZnO: Eu etc.) or different doping concentrations (ZnS: Mn (0.1-5%) are required to achieve tunable color.[3,4,7,9–11,14] Despite the promise of these systems, so far, no study has been reported on tunable emission in visible region in a single sample which at nanoscale can be functionalized for biosensing applications. Recently our group has reported a tunable emission in manganese doped and capped ZnS NPs where single sample of defined concentration emit two colors (orange and green).[17,18] In that case it was achieved by changing excitation wavelength from 215nm to 320nm in organic inorganic doped hybrid nanocomposites. These synthesized samples were used for biosensing applications using fluorescence studies. In order to achieve same property many samples were required earlier with precise control of size or doping.[2,5,7] Cao *et al.*[19] have reported excitation intensity dependent tunable color emissions in CdS/ZnS doped with Mn in single sample where blue and orange colors in a single sample was observed. Here in this article we have used three different concentration of chitosan (CH) for synthesis of ZnS: Mn^{2+} (0.1at. %) NPs. Tunable emission wavelength from blue to yellow orange is achieved by changing excitation wavelength for the same sample. Apart from this an increase in chitosan concentration from 0.01 to 1.0 at. % results ten fold rise in PL intensity along with tunable emission property in same sample. Optimized concentration of capping polymer has been achieved by synthesizing chitosan (0.1, 0.5, 1.0, 1.5, 2.0%) capped ZnS NPs. Chitosan being non toxic and biocompatible polymer possesses tunable emission with ZnS Mn^{2+} NPs which is excitation modulated. Often organic polymers are used to stabilize the NPs and also terminate growth.[15] Here organic polymer is not only stabilizing the NPs but may result charge generation, charge transfer and charge separation at the interface between polymers and NPs.[15,16] Also fluorescence resonance energy transfer (FRET) mechanism is used to explain this new type of tunable emission in singe sample. This work illustrate coupling between Frenkel exciton in organic polymers with wannier exciton in inorganic semiconductors which has been observed for the present nanophosphors and is used for sensing different concentrations of glucose. As glucose level in blood is usually used as a clinical indicator of diabetes, so rapid and accurate determination of glucose in human blood and urine is essential in the diagnosis of diabetes, which is affecting about 150 million people in the world.[20] Based on the enzyme-catalyzed oxidation mechanism glucose oxidase (GOD) has been widely used for optical and electrochemical determination of glucose. Also phosphorescence based detection for blood glucose is reported by tagging ZnS: Mn^{2+} with enzyme GOD.[20] But here in this article we have used biocompatible polymer chitosan for functionalizing ZnS: Mn^{2+} core for sensing of glucose-D. Also tunable emissions from 400nm to 587nm have been reported for same sample with tenfold increase in emission intensity than previously synthesized samples.[18]

II. EXPERIMENTAL SECTION

A. Materials

In the present study, raw materials used for preparing the samples were zinc acetate ($Zn(CH_3COO)_2 \cdot 2H_2O$) (99.99%, Sigma Aldrich), sodium sulphide nonahydrate (99.99%, Sigma Aldrich), chitosan (CH, 99.99%, Sigma Aldrich), Manganese acetate ($Mn(CH_3COO)_2 \cdot 2H_2O$, 99.99%, Sigma Aldrich), double distilled water. All these materials were used without any further purification.

B. Synthesis of CH capped ZnS and CH capped Mn doped ZnS nanocrystals

High purity research grade chemicals purchased from Sigma Aldrich were used without further purification. Chitosan is hydrophilic, nontoxic, biocompatible and biodegradable. CH (0.1-2.0%) capped undoped and CH capped Mn (0.1%) doped ZnS NPs were synthesized by chemical precipitation method as mentioned in our earlier reports.[17,18] In the first step 40mL homogenous solutions of 0.5M zinc acetate, 0.5M sodium sulphide was prepared separately in distilled water by stirring them for half an hour. Also solution of different concentration (0.1, 0.5, 1.0, 1.5, 2.0 at. wt. %) of capping agent (chitosan) used in present investigation was prepared in 40mL solution of 1.0 % acetic acid in distilled water separately. Chitosan is insoluble in water and strong acids but is soluble in dilute acids, as amine group is protonated to NH_3^+. Here we have used 1% acetic acid solution in distilled water to dissolve chitosan. For the synthesis of capped ZnS NPs with various capping concentrations, different sets of 40mL solution of CH (0.1-2.0%) were added slowly in different sets of 40mL solution of 0.5M zinc acetate. All these sets were stirred for half an hour at room temperature. Then to these reaction mixtures 40mL solution of 0.5M sodium sulphide was added drop wise. Soon after the addition of sodium sulphide the precipitation phenomenon occurs and concentration of precipitates increases as addition was increased. For the synthesis of CH (0.01, 0.1, and 1.0 %) capped ZnS: Mn NPs, 0.1% manganese acetate solution was added to zinc acetate solution prior to addition of CH solutions. The procedure following this is same as for undoped NPs and is described above. The solution containing particles (CH capped and doped, CH capped undoped ZnS NPs) were then centrifuged at 4000 rpm for 5 minutes. The precipitated particles were filtered using Whatman 40 filter paper. To remove the last traces of adhered impurities, the particles were washed several times using double distilled water. The washed particles were dried in vacuum oven at 60^{o}C for 24 hours. For comparison of PL intensity and tunable emission property ZnS: Mn^{2+} (0.1at. %) NPs were synthesized with three different concentrations of chitosan (0.01, 0.1, 1.0 at. %). In this study, chitosan was used as surfactant to control the nanocrystal growth and to stabilize the nanocrystals against aggregation. In addition, chitosan was also used to render the nanocrystals water soluble and provide functional chemical groups for further attachment of glucose. For glucose sensing five sets of 0.2 gm of ZnS: Mn^{2+} @ chitosan particles dispersed in 5 mL of Mili-Q water were made. First one is labeled as control. In other four sets 2.5μL, 5μL, 7.5 μL and 10μL of 0.5M glucose-D solution was added and used for further studies.

C. Characterization

The ZnS NPs were characterized by X-ray diffraction (XRD) using Panalytical Xpert Pro MPD with Cu-K_α radiation. TEM micrograph has been recorded using Analytical Transmission electron microscope (FEI model Technai G2-F30) S-Twin having field emission gun with EDS attachment and also having accelerating voltage of 300KV. For TEM study the powder was ultrasonicated in ethanol. One drop of this solution was dropped on carbon coated Cu grid. Ethanol was allowed to evaporate to get finally dispersed powder. Optical absorption of the ZnS particles were recorded with a double beam UV-Visible spectrophotometer (Model: Specord-205) in the 190–1100nm range. PL studies were done with spectrometer (Model: Perkin Elmer55) having slit width of 10nm in all the samples. For all optical studies 0.01gm sample was dispersed in 5 mL of distilled water and further ultrasonicated for half hour to obtain transparent colloidal solutions.

III. RESULTS AND DISCUSSIONS

A. Structural Studies

Fig. 1(a) and 1(b) shows X-ray diffraction pattern of CH (0.1, 0.5, 1.0, 1.5, and 2.0%) capped ZnS and Mn (0.1%) doped, CH (0.01, 0.1, and 1.0%) capped ZnS NPs. It shows three broad peaks corresponding to the (111), (220) and (311) planes of FCC ZnS structure. It is to be noted that, the peaks observed in the XRD pattern match well with those of the β-ZnS (cubic) reported in the ICDD Powder Diffraction files (File. No.80-0020). Lattice spacing (d values) of most intense peak of (111) plane comes out to be 3.09Å. The lattice constant determined from the XRD pattern using

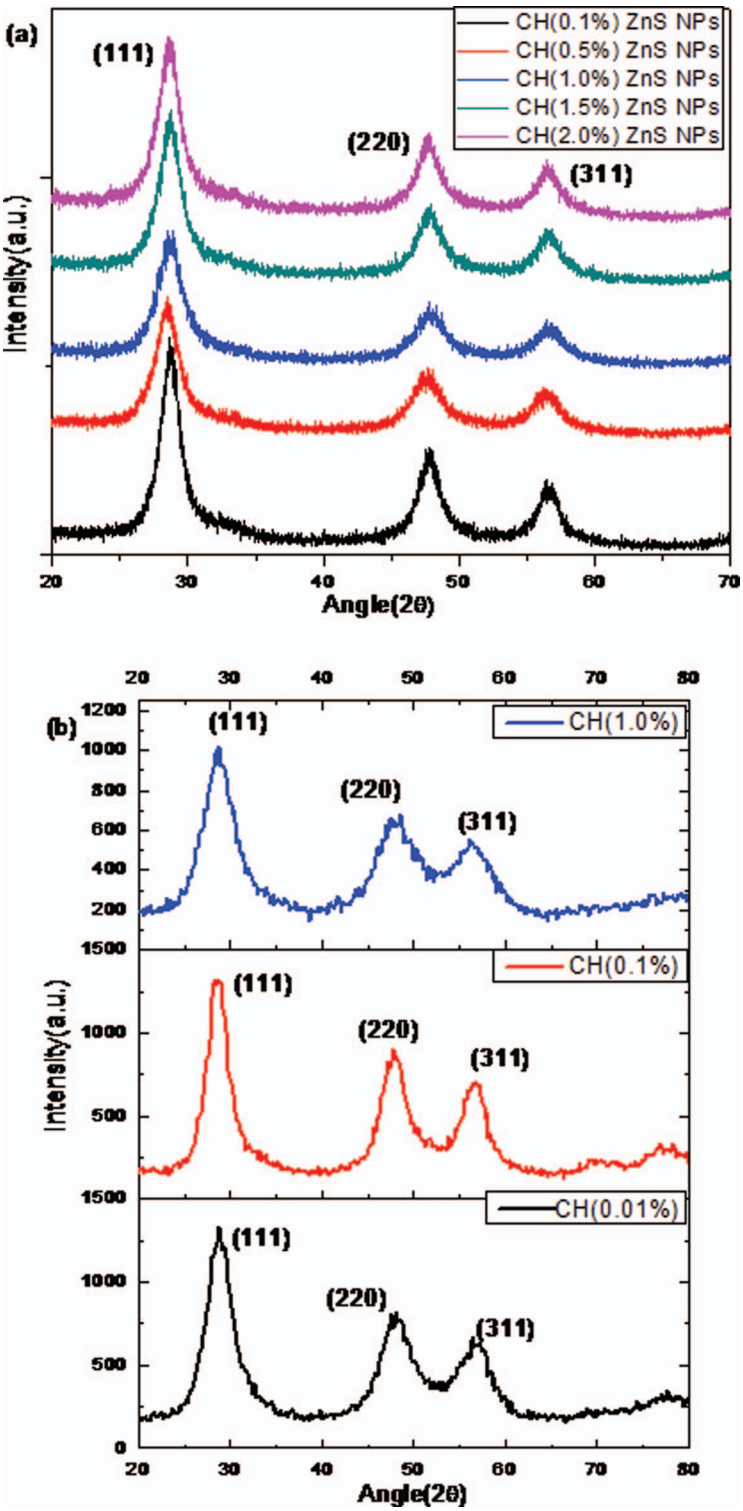

FIG. 1. (a) XRD pattern of CH (0.1-2.0%) capped ZnS NC's (b) CH (0.01-1.0%) capped ZnS:Mn NPs.

(111) plane is a = 5.334 Å, which is close to the reported value of cubic ZnS (JCPDS card, No. 80-0020, a = 5.345Å). Broadening of the XRD peaks indicates the formation of ZnS NC's. The nano crystals have lesser lattice planes compared to bulk which contributes to the broadening of peaks in the diffraction pattern. This broadening is also due to micro straining of the crystal structure which arises from dislocation and twinning.[21] No secondary phase(s) are present in the ZnS: Mn^{2+} NP's. The average crystallite size using Scherer's formula is estimated from three planes is 2.65, 2.55, 2.45, 2.60, 2.64nm for CH (0.1-2.0%) capped ZnS NC's and 2.15, 2.13 and 2.01 nm respectively for CH (0.01, 0.1, 1.0 at. %) capped ZnS: Mn^{2+} NC's. Fig.2(a) shows SEM micrograph of CH (0.1%) capped ZnS:Mn NPs. It shows abundance of spherical particles along with surface present polymer chitosan. Fig.2(b) shows SEM micrograph of CH (1.0%) capped NPs. It shows presence of well separated spherical microspheres of average diameter 2μm (shown in Fig. 2(c)). On the surface of each sphere small particles are adsorbed which show agglomeration by adsorbed polymer. TEM micrograph of CH (0.01%) capped ZnS NPs is showing spherical crystallites of average size 3nm (Fig.S1, Ref.22). Inset of this Fig.S1 shows corresponding SAED pattern showing the presence of three planes. TEM micrograph of CH (0.1%) capped NPs are shown in Fig-3(a) which shows spherical crystallites having mean size ~3.0-4.0 nm. It shows isolated NPs embedded in clusters which are shown in SEM images. Fig-3(b) shows TEM micrograph of CH (1.0 at. %) capped NPs. It shows an abundance of nearly spherical crystallites, which also have a mean particle size of 3.0 nm. Fig. 3(c) represents a magnified HRTEM image of the Mn-doped chitosan (1.0 at.%) capped ZnS NPs with the (111) lattice planes. Magnified HRTEM image of capped NPs is shown in right upper and middle inset. The spacing of the lattice fringes in this HRTEM image is found to be 3.08 Å, which corresponds to the (111) plane of the cubic phase of ZnS which is nearly same as observed in XRD studies as shown above. This is also confirmed from the fast Fourier transform (FFT) pattern of the HRTEM image, as shown in the lower right inset of Fig. 3(c). Fig. 3(d) shows SAED pattern for CH (1.0%) capped NPs. The SAED pattern shows a set of sharp rings corresponding to diffraction from different planes of the nanocrystallites instead of spots due to the random orientation of the crystallites. It is evidently observed three rings corresponding to the (111), (220) and (311) lattice planes of the cubic phase of ZnS, which is in good agreement with the above XRD patterns. Fig.S2 (Ref. 22) shows EDAX pattern of CH (1.0%) capped NPs showing presence of zinc, sulphur and little oxygen and carbon due to polymer.

B. Absorption Studies

Fig-S3 (Ref. 22) shows the absorbance versus wavelength (λ) traces of the CH (0.1- 2.0%) capped ZnS NPs. The absorption spectrum of capped samples show blue shift in absorption shoulder edge as compared to bulk ZnS (340nm) which is due to quantum size effect. Using the Manifacier model,[23] the absorption coefficients (α) were calculated in the region of strong absorption. The values of the band gap were determined by extrapolating the straight line portion of the $(\alpha h\nu)^{1/n}$ versus $h\nu$ graphs to the $h\nu$ axis as shown in Fig-4(a) and Table I. As ZnS is direct band gap material so value of n taken is $\frac{1}{2}$. From the plots the values of band gap were obtained as 3.92, 4.32, 4.65, 4.42 and 4.42eV for CH (0.1, 0.5, 1.0, 1.5, 2.0 at. wt. %) capped ZnS NPs respectively. The results of 1.0% capped sample shows maximum band gap which accounts for high quantum confinement of electrons in this concentration of chitosan. The optical absorption spectra of the CH capped and Mn doped ZnS NPs are shown in Fig-4(b). The absorption spectrum for CH (0.01, 0.1, and 1.0%) capped NP's shows absorption shoulder at 325nm, 325nm and 311nm respectively. Again using the Manifacier model,[23] the absorption coefficients (α) were calculated in the region of strong absorption. The exact values of the band gap were determined by extrapolating the straight line portion of the $(\alpha h\nu)^{1/n}$ versus $h\nu$ graphs to the $h\nu$ axis as shown in Fig-4(c). From the plots the values of band gap were obtained as 4.65eV, 4.73eV and 4.82eV for CH (0.01, 0.1 and 1.0 at. %) capped ZnS: Mn^{2+} NPs respectively. The band gap values were found to increase due to reduced particle size showing strong quantum confinement effect which is higher than the bulk value (340nm of ZnS) having band gap of 3.6 eV.

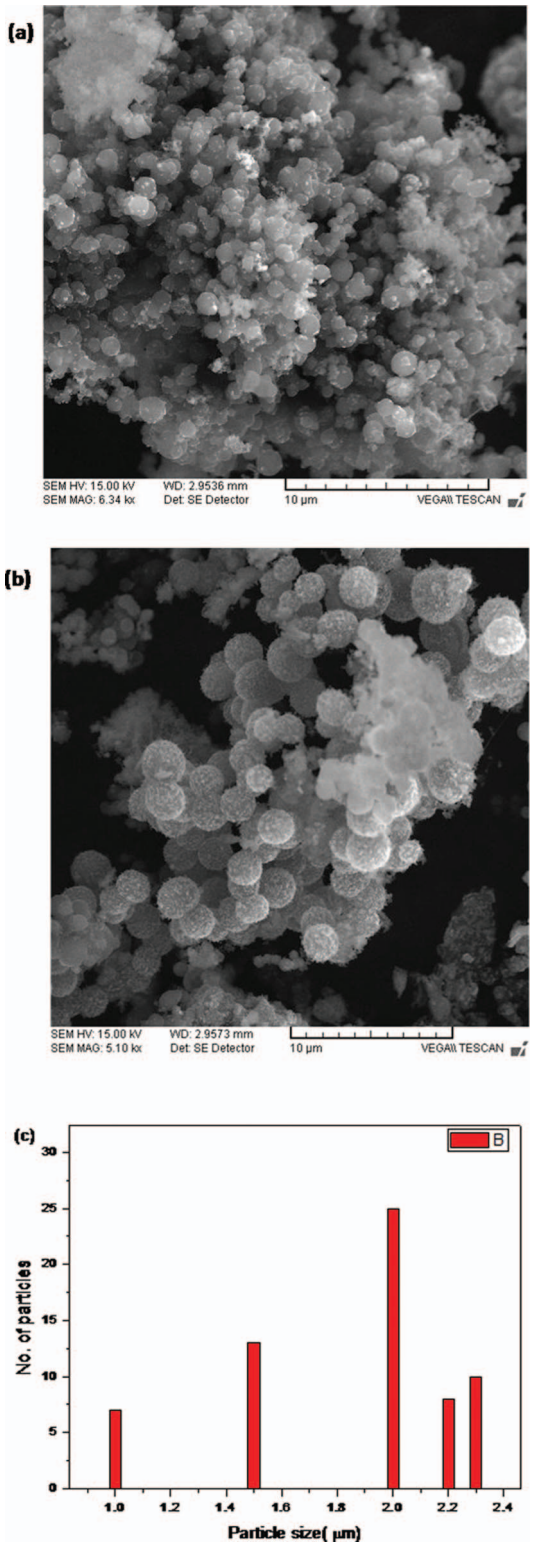

FIG. 2. (a) SEM micrograph of CH (0.1%) capped ZnS:Mn (0.1%) NPs, (b) SEM micrograph of (c) particle size distribution of CH (1.0%) capped ZnS:Mn (0.1%) NPs.

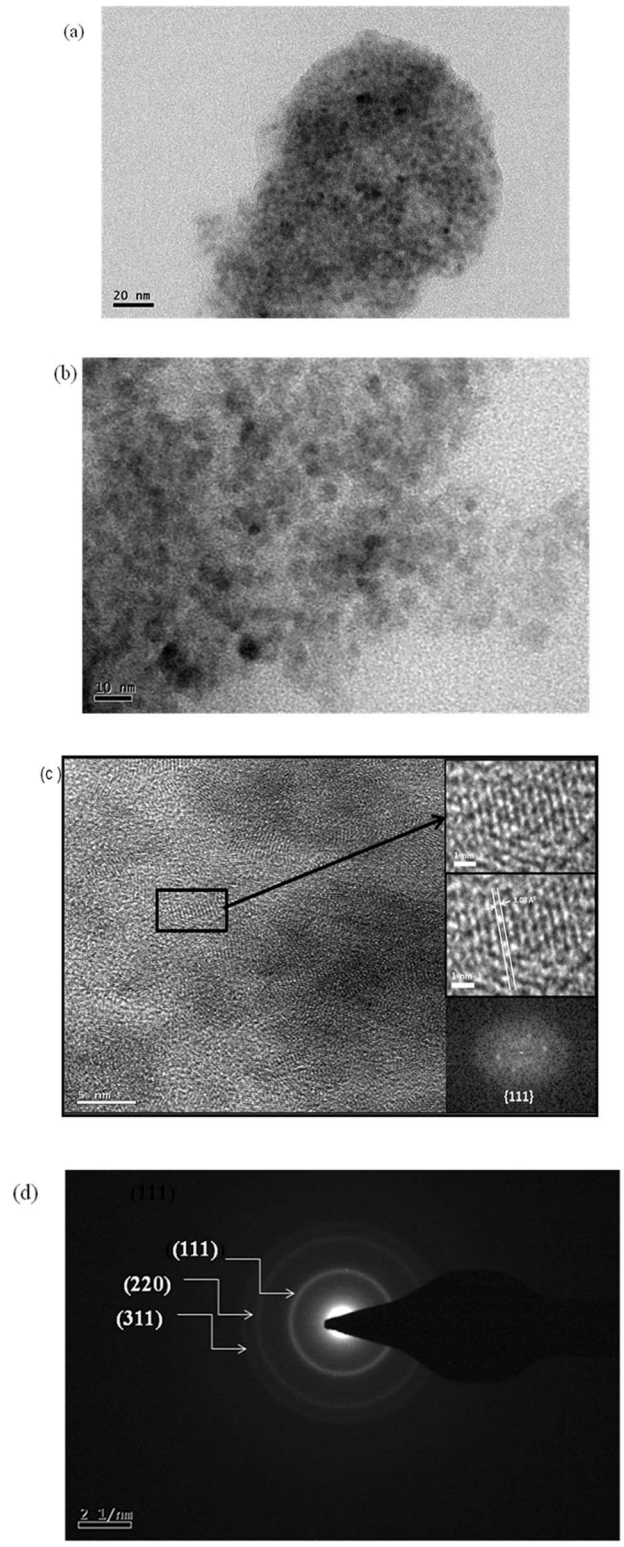

FIG. 3. (a) TEM micrograph of CH(0.01%) capped, (b) CH (1.0%) capped, (c) HRTEM (right upper and middle inset shows magnified HRTEM image showing 0.308nm d spacing, bottom right inset shows FFT pattern of selected HRTEM image), (d) SAED pattern of CH (1.0%) capped ZnS NPs.

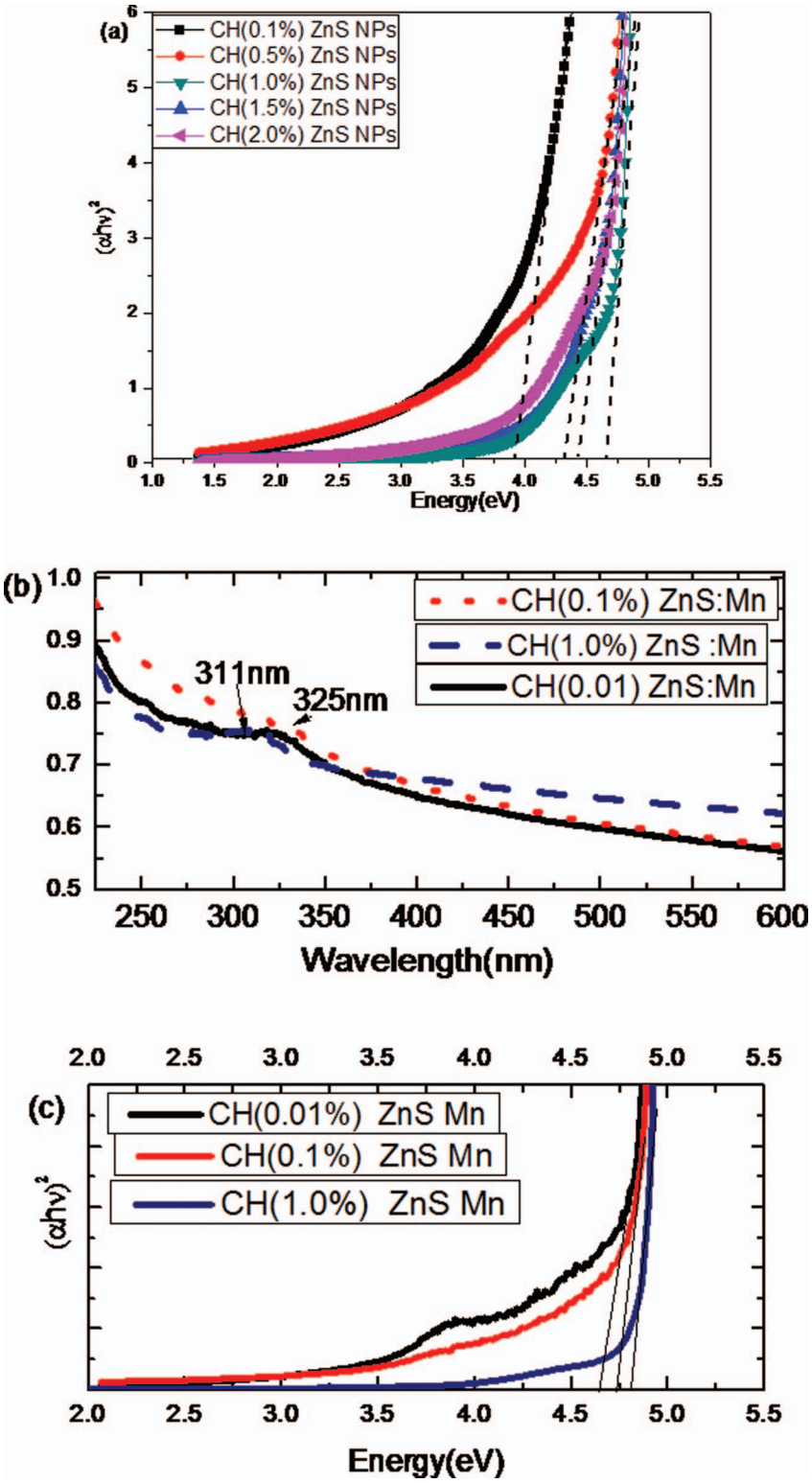

FIG. 4. (a) Estimated band gap by tauc's plot for CH (0.1-2.0%) capped ZnS NPs, (b) Absorbance spectra, (c) estimated band gap by tauc's plot for CH capped ZnS: Mn NPs.

TABLE I. Showing particle size variation of all samples with absorption and photoluminescence results.

Sample	Particle Size (nm) XRD	TEM	Absorption wavelength (nm) UV-Vis. Spectra	Excitation wavelength (nm) 410nm emission	Excitation wavelength (nm) 590nm emission	Band gap (eV) UV-Vis.	PLE	Emission wavelength (nm) 284nm PLE	325nm PLE
CH(0.1%)ZnS NPs	2.65	-	305	280	-	3.92	4.42	395	395
CH(0.5%)ZnS NPs	2.55	-	270	281	-	4.32	4.41	395	395
CH(1.0%)ZnS NPs	2.45	-	276	284	-	4.65	4.36	395	395
CH(1.5%)ZnS NPs	2.60	-	285	282	-	4.42	4.39	395	395
CH(2.0%)ZnS NPs	2.64	-	305	280	-	4.42	4.42	395	395
CH(0.01%)ZnS:Mn(0.1%)NPs	2.15	3-4	325	281*	344*	4.65	-	400, 587	447, 587
CH(0.1%)ZnS:Mn(0.1%)NPs	2.13	3-4	325	284*	298, 340*	4.73	-	400, 587	447, 587
CH(1.0%)ZnS:Mn(0.1%)NPs	2.01	3-4	311	284	298, 318, 325	4.82	4.36	400, 587	447, 587

*Data is not shown in Figures.
Spaces left vacant shows data not collected, not possible or not applicable.

C. Luminescence Studies

Fig.5(a) shows excitation spectra of CH (0.1-2.0%) capped ZnS NPs at fixed emission wavelength of 410nm. It shows excitonic peak centered around 280nm for all CH (0.1-2.0%) concentrations. With increase in concentration of capping agent CH from 0.1-1.0%, intensity of excitonic peak increases and spectra becomes broadened. With further increase in CH from 1.0-1.5 and 2.0% intensity of excitonic peak decreases with slight reduction in broadening. Calculated band gap from excitation spectra are given in Table I for all samples which matches with those calculated with absorption spectroscopy.

Fig. 5(b) shows PL spectra of CH (0.1-2.0%) capped ZnS NPs at 284nm excitation wavelength. Emission peak is observed at 395nm for CH capped ZnS NPs. With increase in capping concentration from 0.1 to 0.5% and further to 1.0% there is increase in emission intensity along with increase in full-width at half maximum. From Table I it is clear that with increase in concentration of capping polymer from 0.1-1.0% there is decrease in crystallite size causing increase in band gap. This increase in PL intensity is due to strong quantum confinement effect and decrease of surface defects with increase in capping agent. The emission observed around 390-410nm results from defect states (sulphur vacancies acting as trap states) which should be further passivated as the amount of capping agent is increased. However, the observed PL intensity of defect states increases surprising (for 0.1-1.0% CH). Moreover, with further increase in CH concentration from 1.0-1.5 and 2.0 % emission intensity observed is decreased. This decrease is probable because the increased capping concentration leads to partially passivation of zinc defects, resulting in decrease of their characteristic emission. It is reported in our previous paper[18] and later on (Fig. 6(d)) in this article that pure chitosan shows broad emission around 350-450nm having maxima at 357nm. So with increase in chitosan concentration from 0.1-0.5 and 1.0% increase in PL intensity can be attributed to convolution of chitosan emission with defect related emission around 410nm. It is reported earlier that 410nm peak in ZnS is due to transfer of electrons from sulphur vacancies acting as trap states to zinc defects.[7, 10, 18, 24] It is possible that for 1.5% and 2.0% CH sample, zinc defects are passivated resulting in elimination of its corresponding peak at 410nm. This might have slightly decreased the integrated emission around 395nm in this case. The adsorbed polymer lies on surface of NP and due to high surface to volume ratio at nano regime more defects would lie on surface so sufficient amount of polymer can passivate defects causing decrease in emission intensity of 410nm peak for 1.5 and 2.0 % CH. Since we wish to achieve tunable emission color in single sample and 1.0% CH capped NC's show maximum PL intensity for 395nm emission so for further PL studies with capping and doping both, this concentration of CH is selected. As for higher concentration of CH (1.5-2.0%) there is decrease in blue color intensity so that samples after doping (Mn) could only give orange color which is well reported in literature.[7, 10, 24]

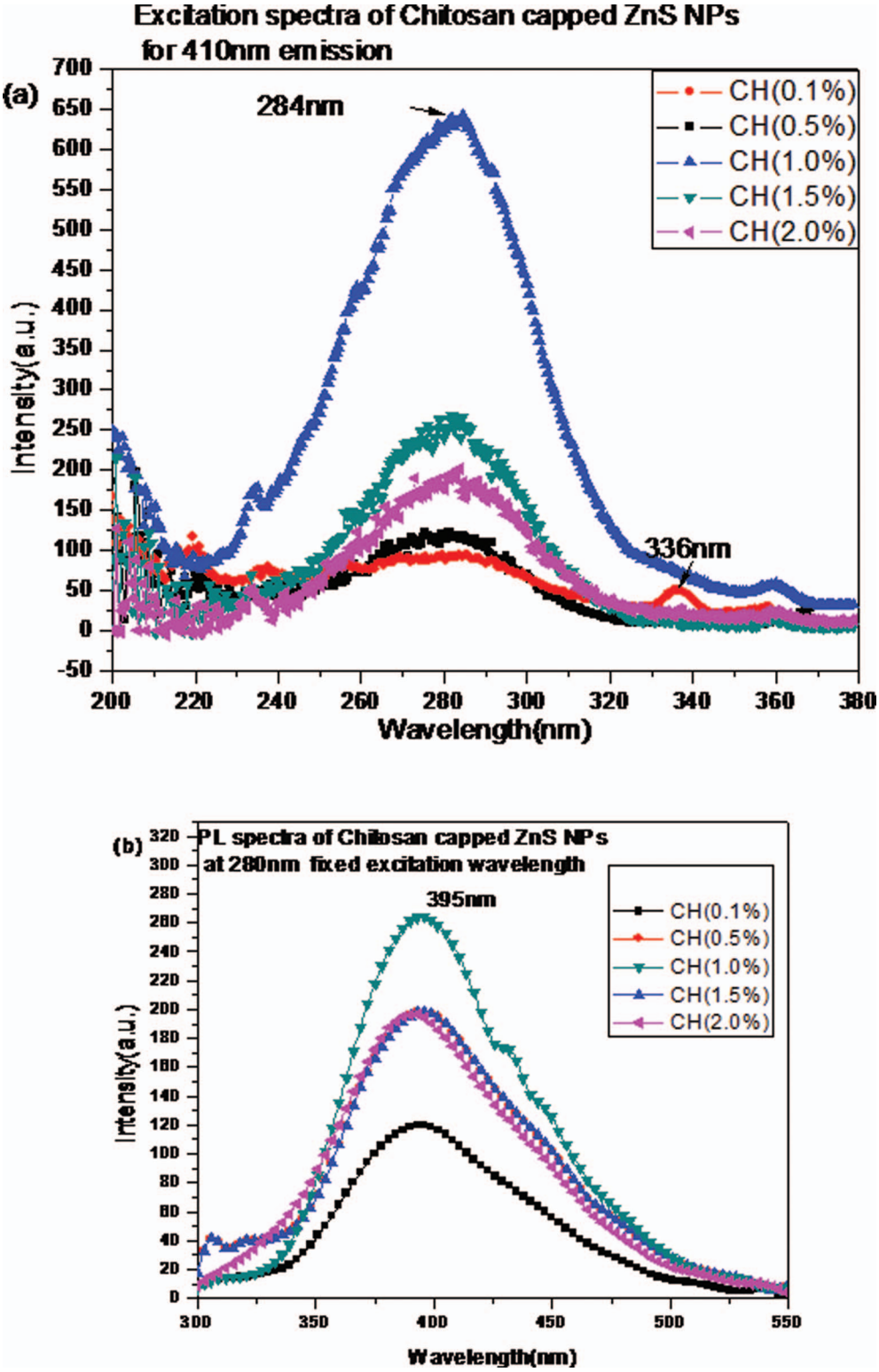

FIG. 5. (a) Excitation spectra (b) Emission spectra of of CH (0.1-2.0%) capped ZnS NPs.

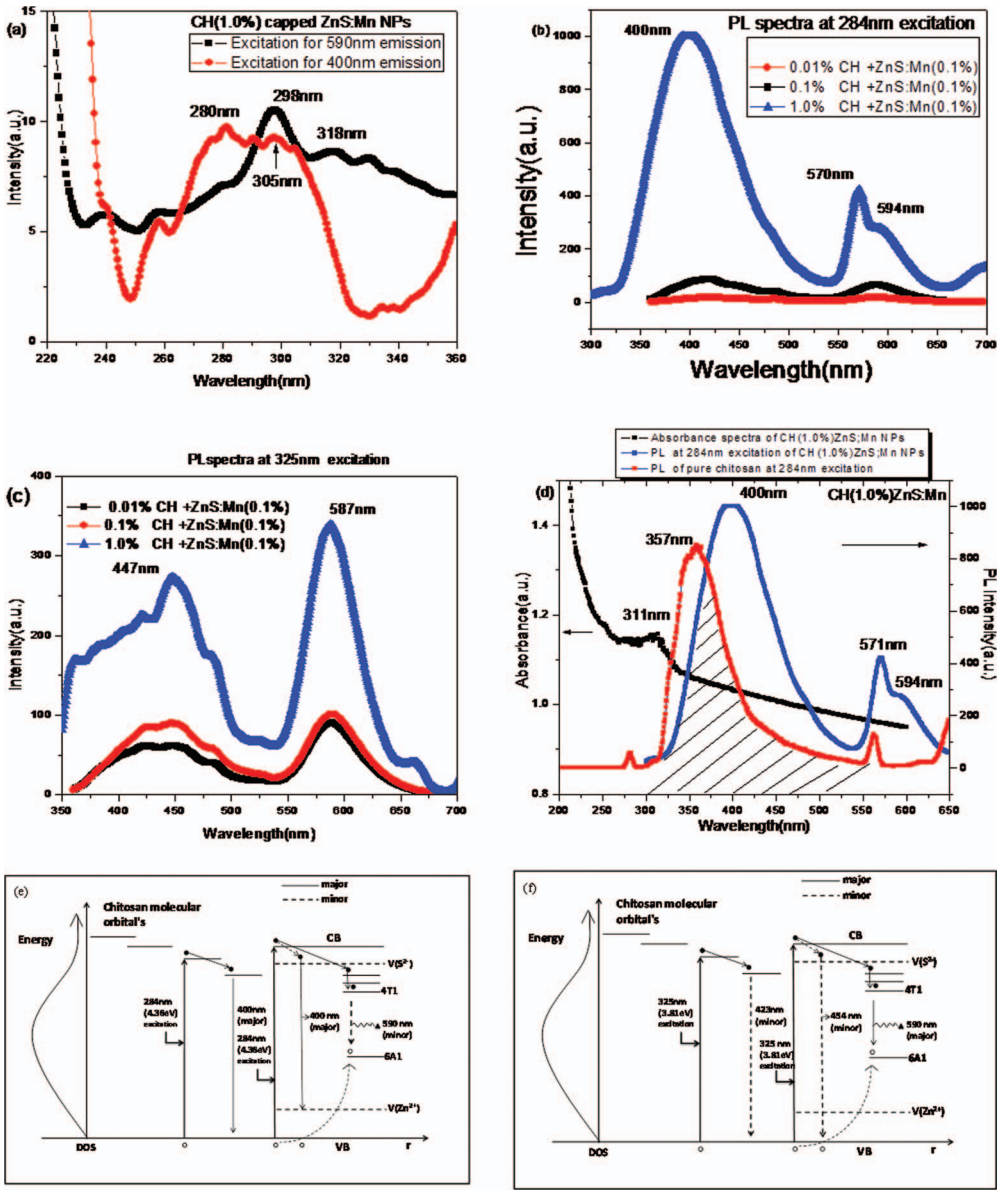

FIG. 6. (a) Excitation spectra of CH capped ZnS Mn NPs. (b, c) PL spectra of chitosan (CH) capped ZnS: Mn at different excitation wavelengths. (Excitation wavelength and sample specifications are written as an inset for each case) (d) FRET mechanism with absorption and PL spectra (e) Energy transfer mechanism for CH capped ZnS: Mn NPs at 284nm excitation (f) Energy transfer mechanism for CH capped ZnS: Mn NPs at 325nm excitation.

Fig-6(a) shows excitation spectra of CH (1.0%) capped ZnS: Mn^{2+} NC's for two possible emissions (400, 590nm). For emission in range of 400nm excitation spectra is broadened in comparison to undoped CH (1.0%) ZnS NPs showing highest excitonic peak at 280nm along with weak peaks at 305nm, 330nm respectively. This broadening can be attributed to more energy states present in doped and capped sample in comparison to undoped and capped sample. Further for Mn dopant related emission (590nm), the PLE spectra exhibit red shifts from 284nm to 298nm and 318nm. This shows that in doped sample there are two possible emission sites for emission. As excitonic peak around 284nm is observed for undoped samples also so it can be responsible for 410nm emission due to trap states and 350-400nm emission due to chitosan. Also excitonic peak around 298-330nm results for 590nm emission so this shows that emission spectra would be dependent on excitation wavelength.

TABLE II. showing relative emission intensities of blue and orange color along with CIE coordinates.

	$I_{400/587}$ (blue/orange)		CIE coordinates		Color O/P	
	For 284nm	For 325nm	For 284nm	For 327nm	For 284nm	For 325nm
Sample	PLE	PLE	PLE	PLE	PLE	PLE
CH (0.01%) ZnS: Mn (0.1%) NPs	1.11	0.66	-	-	Blue	Orange
CH (0.1%) ZnS: Mn (0.1%) NPs	1.35	0.85	-	-	Blue	Orange
CH (1.0%) ZnS: Mn (0.1%) NPs	3.59	0.79	(0.273, 0.20)	(0.344, 0.275)	Blue	Orange

*Data is not shown in Figures.
Spaces left vacant shows data not collected, not possible or not applicable.

In order to further explain these dual excitonic peaks for same sample in excitation spectra, emission spectra were recorded for all doped and undoped samples at two different excitation wavelengths (284, 325nm).

Fig-6(b) and 6(c) shows a comparison study of PL spectra of these ZnS: Mn^{2+} NP's at two different excitations (284, 325nm). The spectra were recorded at an emission filter at 290 and 350nm for corresponding excitation wavelength of 284 and 325nm. Fig 6(b) shows PL spectra of chitosan capped ZnS: Mn NPs at 284nm excitation wavelength showing emission at 400nm in all the samples. This emission corresponds to the self activated blue emission near band edge emission which is due to radiative transition from the sulphur vacancies (V_s) to zinc defects[24–26] and adsorbed chitosan on host ZnS surface (discussed later). Emission at 587 nm is due to $^4T_1$ - $^6A_1$ transitions in dopant Mn^{2+} energy levels.[6,10,24,25] As shown in Fig 6(b) and 6(c) an increase in integrated PL emission intensity is observed with increase in capping concentrations from 0.01-1.0at % for both excitations. This rise in PL intensity is also observed for undoped CH (0.1-2.0%) ZnS NPs which is due to presence of chitosan emission for same excitation conditions. So, for further study we have used CH (1.0%) capped sample only.

It is observed in Fig.6(b) that for excitation wavelength of 284nm, emission spectrum is broad having two peaks at 400nm and 587nm. Emission intensity of 400nm peak is higher than 587nm peak which is calculated and presented in Table II. However, at 325nm excitation, emission corresponding to 400nm is quenched and 590nm is enhanced for the same sample (Fig-6(c)). This shows single sample (CH 1.0 at. % ZnS: Mn^{2+}) is emitting two different colors at different excitations. For understanding the possible influence of chitosan on PL intensity of doped QDs, the fluorescence of chitosan was investigated. Using 284nm excitation wavelength a broad fluorescence spectrum (300-500nm) with peak centered at 357nm was observed for pure chitosan (Fig-6(d)). Since the emission spectrum of chitosan was observed to overlap with the absorption band of QDs, the fluorescence resonance energy transfer (FRET) should be taken into account to explain excitation induced tunable emission in our case. The enhancement in fluorescence of QDs with increase in concentration of chitosan (0.01 to 1.0at. wt. %) was more pronounced for 400nm emission in comparison to 587nm emission. This can be explained by two mechanisms. First effective FRET is taking place (from adsorbed chitosan to ZnS) in case of 400nm emission as compared to 587nm emission. This is because the absorption spectra of QDs (around 300-350nm) is overlapping to some extend with emission spectra of chitosan (300-500nm) causing enhancement of emission at 400nm instead of 590nm (Fig-6(d)). Second possibility exists in case of overlapping of emission spectra of pure chitosan (which is broad and centered on 357nm) with emission spectra due to sulphur vacancy (which is also broad and centered around 420nm[7,26]). It is shown by shaded portion in Fig. 3(c). Because of high surface to volume ratio, more vacancy exists at surface which gets partially passivated by adsorbed chitosan. This creates an atmosphere of vacancy and defects at the surface. This behavior is also observed for CH (0.1-1.0%) capped undoped ZnS NPs which is discussed above. As per published work[24–27] if Mn^{2+} ions are substituted outside the ZnS crystal then emission peak at 350nm appear instead of 430 and 590nm. Since this type of behavior is not observed in our case (Fig.6(c)) so, it can be concluded that Mn^{2+} ions are doped at interstitial sites of host ZnS NPs. According to foster theory[9] energy transfer is dependent on spatial distance between donor and acceptor. In all the samples sulphur vacancies exist at the surface giving rise to Zn dangling bonds which forms shallow

donor levels. As these dangling bonds are lying at surface of quantum dots so there can be strong coupling between defect states and capping polymer. The distance between adsorbed chitosan and interstitially existing Mn^{2+} ions is more as compared to sulphur vacancy which is existing at surface. Because of this the effective energy transfer (based on Foster theory) would take place from chitosan molecular energy levels to defect states which get further enhanced with increase in concentration of chitosan (0.01 to 1.0%) on surface (Fig-6(b) and 6(c)). Kong *et al.*[28] have also studied effect of distance between acceptor and donor on optical properties of composite semiconducting polymer films. They have shown that energy transfer efficiencies calculated from time resolved PL spectra are consistent with calculated from emission spectra of donor with and without acceptor. The energy transfer efficiency from adsorbed chitosan to host ZnS and chitosan to dopant Mn can be calculated from emission occurring from donor (chitosan) in the absence and presence of acceptor(ZnS:Mn QDs), which can be written in the following form:

$$\Phi_T = 1 - \frac{\int_0^\infty I_D(\lambda)d\lambda}{\int_0^\infty I_D^0(\lambda)d\lambda} \quad (1)$$

where, $I_D^0(\lambda)\,d\lambda$ and $I_D(\lambda)\,d\lambda$ are the PL intensities of chitosan without ZnS: Mn and with ZnS:Mn, respectively, at the emission wavelength of λ(nm). It can be calculated from PL spectra of pure chitosan without ZnS:Mn and with ZnS:Mn in Fig. 6(d) that energy transfer efficiency from chitosan to ZnS :Mn for 284nm excitation is 55.8%. Also following the same procedure energy transfer efficiency from chitosan to dopants for 325nm excitation comes out to be 40.0% which is less than for 284nm excitation. These studies suggest that if molecular energy levels of chitosan are excited then emission is obtained from defect states of ZnS and not from dopant sites (Fig.6(b)). Fig-6(c) shows second case for same capped sample where dopant related emission (587nm) is enhanced and defect related emission (∼400nm) is partially quenched, when excitation wavelength is 325nm i.e. near conduction band of ZnS. Fig.6(e) and 6(f) shows energy transfer mechanism for two possible emissions (400nm, 587nm) corresponding to 284nm and 325nm excitations in single sample respectively. In our previous paper[18] we have shown preliminary results for excitation induced tunable emission in CH (0.01, 0.1 at %) capped ZnS: Mn^{2+} NP's. But there excitation wavelength required for getting two emission colors were 215 and 320nm respectively. The exact concentration required for getting enhanced emission with tunable property was not done. Also for 215nm excitation multiple emission peaks at 421 and 486nm (green color) along with some small peaks were observed. But here we report broad peak centered at 400nm (for 284nm excitation) due to sulphur vacancies and adsorbed chitosan with tenfold rise in emission intensity in comparison to previously synthesized samples. Also for 325nm excitation, dopant (Mn^{2+}) related emission peak at 587nm is greatly enhanced (four fold) than reported earlier.[18] Here in this article we have optimized capping concentration for achieving high emission intensity and at the same time dual emission is achieved at this concentration in same sample. As shown in Fig.6(c) we have also observed broad emission peak at 450nm along with 587nm, which corresponds to sulphur vacancy related emission. But for (1.0 at. %) CH capped ZnS:Mn^{2+} NP's 587nm emission peak is sharp and slightly higher in intensity than 450nm peak although concentration of Mn^{2+} is same in all samples. This shows better coupling of sp states of ZnS with $3d^5$ levels of Mn^{2+} instead of defect states of ZnS NPs. Bhargava *et al.*[13] reported that in Mn^{2+} doped ZnS NP's, very strong hybridization occurs between the sp levels of zinc and d levels of Mn^{2+} ions which results in crystal field splitting of Mn^{2+} levels in between the bands of host material. Subsequent transfer of excited electrons from CB to Mn^{2+} levels and further transition between $^4T_1$ - $^6A_1$ leads the emission of orange color. Secondly at 325nm excitation wavelength, energy states of adsorbed polymer are not excited which otherwise could have given emission at 400nm.

So, the emission observed in our case is different than reported previously[7,10] because we are getting energy transfer in two different ways. In the first case energy transfer takes place from molecular energy levels of capping agent to defect states where dopant related emission is quenched, which according to earlier reports is enhanced.[7] In second case for same sample at different excitation wavelength energy transfer takes place from ZnS band states to Mn^{2+} d levels giving orange emission as shown in Fig-6(c) and defect related emission is quenched.

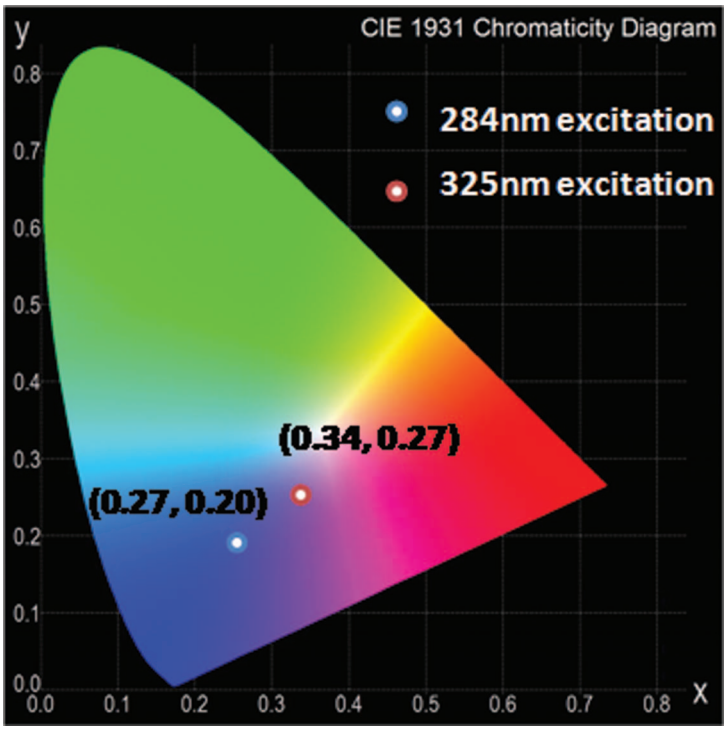

FIG. 7. Showing CIE color coordinates of CH (1.0%) capped ZnS:Mn NPs at two different excitation wavelengths.

Table II shows $I_{400/587}$ (blue/orange) ratio for all doped and capped samples. For CH (1.0%) capped ZnS:Mn sample it comes out to be 3.59, which shows, this sample emits intense blue color instead of orange (expected for Mn doped ZnS) at 284nm excitation. Fig.S 4(a) shows digital picture of this sample excited by UV lamp at high energy (low wavelength). This shows intense blue emission at this excitation. Corresponding Commission Internationale de I' Eclaerage (CIE) color coordinates for this same sample at 284nm excitation as shown in Table II and Fig.7 are (0.273, 0.200) suggesting blue emission. $I_{458/587}$ (blue/orange) for 325nm excitation wavelength comes out to be 0.79 (less than one) showing orange color dominant emissions (Table II). Fig-S 4(b) shows orange color emitting NC's excited with UV lamp having lower excitation energy. There the corresponding CIE color coordinates comes out to be (0.344, 0.275) are shown in Fig. 7 and Table II. The CIE color coordinates corresponding emission spectra (Fig. 6(b) and 6(c)) are shifted from (0.273, 0.200) to (0.344, 0.275) for single sample with shift in excitation wavelength. This clearly shows by changing excitation energy in this hybrid CH (1.0%) capped Mn doped ZnS NC's sample we can manipulate the relative emission intensities of blue light and orange light. This results in a tunable color output in visible region for a single sample. It is important to note that this kind of tunable emission is also reported for ZnS: Mn NPs having different concentrations of Mn.[5] Secondly this is achieved by doping different transition metal ions (Mn, Cu, Eu etc.) in host ZnS or varying particle size of same sample.[7,10] But here in this paper we report same tunable emission but in single sample instead of many samples. It is important to mention here that peak position is not shifted but their emission intensities are changed with shift in excitation energy from 284nm to 325nm respectively resulting in shift of emission color from blue to orange in same NC sample.

D. Glucose Sensing

The observed tunable emission property is greatly enhanced with more specific emission color w.r.t. fixed excitation in CH (1.0%) capped NPs. Since these synthesized CH (1.0 at. %) capped NPs (single sample) are emitting two colors. So in the present study it is used for sensing of glucose. As mentioned above in experimental section five sets were made for sensing studies of glucose with

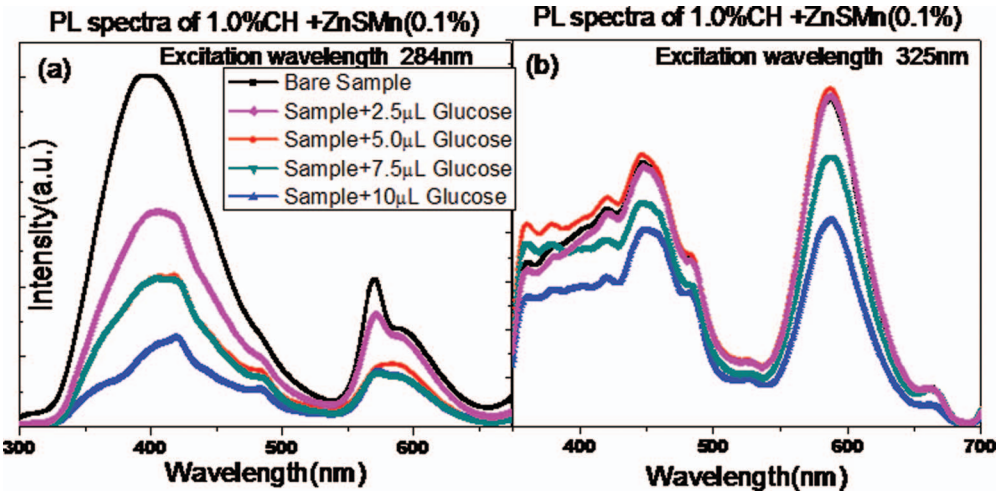

FIG. 8. (a, b) Glucose detection by change in PL intensity of Chitosan capped ZnS Mn NPs at 284nm and 327nm excitation.

capped NP's. Though our PL studies exhibit multicolor emission from single sample but sample exhibiting high PL intensity (CH-1.0% capped NPs) has been selected for possible application in future glucose-D sensing. Solution of glucose doesnot shows any considerable emission in the studied emission range (400-600nm) of CH capped ZnS: Mn^{2+} NPs (Fig.S5, Ref. 22). Fig-8(a) and 8(b) shows PL intensity response of CH (1.0at. %) capped ZnS: Mn^{2+} at 284 and 325nm excitation with different concentration (0-10μL) of glucose–D. Quenching of PL intensity of NP's was observed with increasing glucose concentration from 0-10 μL. This quenching of PL peak for 284nm excitation is more pronounced than for 325nm excitation as shown in Fig 8(a) and 8(b). This can be due to attachment of glucose with surface defects and adsorbed chitosan which will affect its luminescence peak at 400nm. The emission at 400nm for capped ZnS: Mn^{2+} NPs is due to surface defects and 587nm is due to Mn^{2+}. Also Mn^{2+} ions are incorporated inside the host ZnS at interstitial sites so interaction of Mn^{2+} with glucose is less probabilistic than with surface adsorbed chitosan and excess Zn^{2+} ions. So there is non- uniform quenching of PL intensity due to dopant related emission (587nm). It indicates that variation in PL intensity with concentration of surface adsorbed glucose is more at 284nm excitation having 400nm emission. When glucose is added there is change in surface of capped ZnS NPs. This is due to interactions between glucose and surface polymer (chitosan) which are shown in FigS6. These interactions may be due to: formation of hydrogen bond between N of chitosan and H of glucose, formation of hydrogen bond between O of chitosan and H of glucose, formation of O-glycosidic linkage between glucose and chitosan and formation of N-glycosidic linkage between glucose and chitosan. Further research on the detailed mechanism of glucose sensing with CH capped NPs is being carried out.

IV. CONCLUSIONS

We have shown a shift in PL emission spectra from orange to blue in chitosan capped Mn-ZnS sample. Our studies suggest that different colors in visible range can be observed in a single organic-inorganic hybrid sample with change in excitation wavelength. Earlier it is reported that only PL intensity varies if excitation wavelength is changed. But here we have shown multicolor emission in single sample with enhanced PL intensity. Energy transfer mechanism from donor to acceptor states based on resonance energy transfer has been discussed in detail. The intensity of emission peak around 400nm is having ten fold rise as compared to previously reported values. CIE color coordinates shows shifting from (0.273, 0.200) to (0.34, 0.275) with variation in excitation energy showing tunable color characteristics in single sample. In all previous cases many samples with controlled synthesis procedures are required but in our case it is observed in single sample which will be useful for different more stable and efficient light-emitting devices in optoelectronics

and biosensors. At last we have also shown preliminary results showing glucose sensing with biocompatible chitosan capped manganese doped ZnS NP's and compared their results for two possible emission (400, 587nm) sites of same sample.

ACKNOWLEDGMENT

The authors are thankful to Defense Research Development Organization, Government of India for providing financial assistance vide project no. ERIPR/ER/0703659/M/01/1287 for carrying out this work.

[1] D. Denzier, M. Olschewski, and K. Sattler, J. Appl. Phys. **84**, 5 (1998).
[2] C. B. Murray, D. J Norris, and M. G Bawendi, J. Am. Chem. Soc. **115**, 8706 (1993).
[3] C. H. Fischer, E. J. H. Hart, and A. Henglein, Ber. Bunsenges. Phys. Chem. **90**, 46 (1986).
[4] C. H. Fischer, J. Lilie, H. Wellerm, L. Katsikas, and A. Henglein, Ber. Bunsenges. Phys. Chem C. B. **93**, 61 (1989).
[5] Z. Quan, D. Yang, C. Li, D. Kong, P. Yang, Z. Cheng, and J. Lin, Langmuir **25**, 10259 (2009).
[6] N. Murase, K. Hirata, T. Yazawa, and T. Kushida, J. Phys. Chem. B. **103**, 754 (1999).
[7] K. Manzoor, R. Vadera, N. Kumar, and T. R. N. Kutty, Solid State Communications **129**, 469 (2004).
[8] R. Chen Wei Sammynaiken, Y. Huang, Jan-Olle Malm, Reine. Wallenberg, Zwiller. Bovin Jan-Olov, Kotov. Valery, and A. Nicholos, J. Appl. Phys. **89**, 1120 (2001).
[9] Scherf. Stoferle Thilo, Mahrt. Ullrich, and F. Rainer, Nano lett. **9**, 453 (2009).
[10] S. Sapra, A. Prakash, A. Ghangrekar, N. Periasamy, and D. D. Sarma, J. Phys. Chem. B. **109**, 1663 (2005).
[11] J. E. B. Katari, V. L Colvin, and A. P Alivisatos, J. Phys. Chem. **98**, 4109 (1994).
[12] R. Maity and K. K. Chattopadhyay, Nanotechnology. **15**, 812 (2004).
[13] R N. Bhargava, J Lumin. **70**, 85 (1996).
[14] S. C Erwin, Zu, L. M. I Haftel, A. L. Efros, T. A. Kennedy, and D. J Norris, Nature (London) **436**, 91 (2005).
[15] W. Chen, A. G. Joly, J.-O. Malm, J.-O. Bovin, and S. Wang, J. Phys. Chem. B **107**, 6544 (2003).
[16] H. Wei, H. Sun, H. Zhang, C. Gao, and B. Yang, Nano Res. **3**, 496 (2010).
[17] M. Sharma, S. Kumar, and O. P. Pandey, J Nanopart. Res. **12** (7), 2655 (2010).
[18] M. Sharma, S. Singh, and O. P. Pandey. J. Appl. Phys. **107**, 104319 (2010).
[19] O. Chen, D. E. Shelby, Y. Yang, J. Zhuang, T. Wang, C. Niu, N. Omenetto, and Y. C. Cao, Angewandte Chemie International Edition **49**, 10132 (2010).
[20] Wu P. He Yu. Wang, He-Fang, and Yan Xiu-Ping, Anal. Chem. **82**, 1427 (2010).
[21] H. C. Warad, S. C. Ghosh, B. Hemtanon, C. Thanachayanont, and J. Dutta, Sci Technol Adv Mater. **6**, 296 (2005).
[22] See Supplementary material at http://dx.doi.org/10.1063/1.3698310 for [SEM micrograph of CH (0.1%) capped ZnS:Mn(0.1%) NPs, TEM micrograph of CH (0.01%) capped ZnS: Mn NPs, Absorption spectra of CH (0.1-2.0%) capped ZnS nanoparticles, Digital images of CH (1.0%) capped ZnS:Mn (0.1%) NP's under UV lamp, PL spectra of glucose with chitosan, Sensing mechanism of glucose D with chitosan capped ZnS:Mn^{2+} NP's].
[23] J. I. Pankove, *Optical Processes in Semiconductors* (Prentice-Hall, Englewood Cliffs, NJ, 1971).
[24] K. Sooklal, B. S. Cullum, S. M. Angel, and J. Murphy, J. Phys. Chem. **100**, 4551 (1996).
[25] R. Sarkar, C. S. Tiwary, P. Kumbhakar, S. Basu, and A K. Mitra, Physica E. **40**, 3115 (2008).
[26] J. F. Suyver, S. F. Wuister, and J. J. Kelly, Nano Lett. **1**, 429 (2001).
[27] M. R. Kim, J. H. Chung, and D. J. Jang, Phys. Chem. Chem. Phys. **11**, 1003 (2009).
[28] F. Kong, J. Liu, X. Zhang, Y. An, X. Li, B. Lin, and T. Qiu, J. Lumin. **131**, 815 (2011).